THE JOURNAL OF PHYSICAL CHEMISTRY B

Article

pubs.acs.org/JPCB

Systematic Investigation on the Central Metal Ion Dependent Binding Geometry of M-*meso*-Tetrakis(*N*-methylpyridinium-4-yl)porphyrin to DNA and Their Efficiency as an Acceptor in DNA-Mediated Energy Transfer

Young Rhan Kim,[†] Lindan Gong,[†] Jongjin Park,[†] Yoon Jung Jang,[†] Jinheung Kim,[‡] and Seog K. Kim*[,†]

[†]Department of Chemistry, Yeungnam University, Dae-dong, Gyeongsan City, Gyeong-buk, 712-749, Republic of Korea

[‡]Department of Chemistry and Nano Science, Ewha Womans University, Seoul, 120-750, Republic of Korea

ABSTRACT: Binding geometry to DNA and the efficiency as a donor for energy transfer of various metallo- and nonmetallo-porphyrins were investigated mainly by polarized light spectrscopy and fluorescence measurements. Planar porphyrins including nonmetallo *meso*-tetrakis(*N*-methylpyridinium-4-yl)porphyrin (TMPyP), CuTMPyP, and NiTMPyP produced large red-shift and hypochromism in absorption spectrum and a negative circular dichroism (CD) in the Soret band suggesting that these porphyrins intercalate between DNA base-pairs as expected. In the intercalation pocket, the molecular plane of these porphyrins tilts to a large extent. From a linear dichroism (LD) study, the angle between the two electric transition moments in the Soret band were 16°, 12°, and 11° for TMPyP, NiTMPyP, and CuTMPyP, respectively. On the other hand, porphyrins with axial ligands namely, VOTMPyP, TiOTMPyP, and CoTMPyP, produced a positive CD signal in the Soret band. Hyperchromism and less red-shift were apparent in the absorption spectrum. These observations indicated that the porphyrins with an axial ligand bind outside of the DNA. The angles of both the B_x and B_y transition with respect to the local DNA helix were 39°~46° for all porphyrins. From these results, the conceivable binding site of porphyrins with axial ligands is suggested to be the minor groove. All porphyrins were able to quench the fluorescence of intercalated ethidium. Strong overlap between emission spectrum of ethidium and the absorption spectrum of porphyrins when they simultaneously bound to DNA was found suggesting the mechanism behind energy transfer is, at least in part, the Förster type resonance energy transfer (FRET). The minimum distance in base pairs between ethidium and porphyrin required to permit the excited ethidium to emit a photon was the longest for CoTMPyP being 17.6 base pairs and was the shortest for CuTMPyP and NiTMPyP at 8.0 base pairs. The variation in the distance was almost proportional to the extent of the spectral overlap, the common area under emission spectrum of ethidium and absorption spectrum of porphyrin, supporting the FRET mechanism, whereas the effect of the orientation factor which was considered by relative binding geometry was limited.

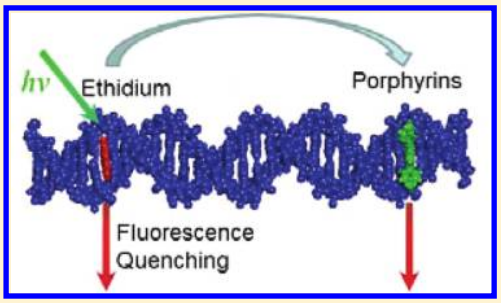

INTRODUCTION

Cationic porphyrins bind to various forms of DNAs. Interaction of cationic porphyrin with DNA has been widely studied since the pioneering work of Pasternack[1] and Fiel,[2−4] due to their unique physicochemical aspect of the complex formed with DNA and to potential application for medicinal-chemistry and biology. In regard to the medicinal and biological applications, porphyrins have been used in photodynamic therapy,[5−7] cancer detection,[8,9] virus inhibition,[10,11] and artificial nuclease.[12,13]

Several binding modes of cationic porphyrin to native and synthetic DNA have been reported including intercalation,[14−17] groove binding,[17−24] outside random binding,[25−27] as well as moderate and extensive stacking.[27−39] These binding modes are affected by a variety of factors namely, the structure of periphery groups, the number and position of the positive charges, the nature of DNA bases, morphology and length of DNA, the nature of a central metal ion and the salt concentration of the medium. One recent example showed that position and number of positive charges of cationic porphyrins drastically changed the binding mode of porphyrins to double stranded native DNA, poly[d(G-C)$_2$] and poly[d(A-T)$_2$].[40,41] *meso*-Tetrakis(*N*-methylpyridinium-4-yl)porphyrin (herein denoted as TMPyP, Figure 1), a representative member of the porphyrin family, has been intercalated between the base-pairs of native DNA and poly[d(G-C)$_2$] at low [porphyrin]/[DNA] ratios (referred to as the *R* ratio). It seems to bind across the minor groove of poly[d(A-T)$_2$]. As the porphyrin concentration increased, TMPyP started to stack along the DNA, poly[d(G-C)$_2$] and poly[d(A-T)$_2$]. In contrast, *cis*-bis(*N*-methylpyridinium-4-yl)porphyrin, where the number of positive charges is reduced to two, does not intercalate. It stacked along the DNA and polynucleotide stem. The nature of the central metal ion of the metallo-porphyrins is another important factor in determining the binding mode of cationic

Received: December 20, 2011
Revised: January 21, 2012
Published: January 23, 2012

   dx.doi.org/10.1021/jp212291r | *J. Phys. Chem. B* 2012, 116, 2330−2337

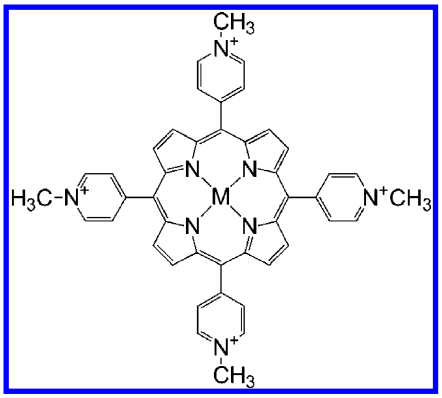

Figure 1. Chemical structure of M-*meso*-tetrakis(*N*-methylpyridinium-4-yl)porphyrin (MTMPyP). The central metal ions investigated in this work are metal-free TMPyP, Cu(II), Ni(II), V(IV)=O, Ti(IV)=O and Co(III).

porphyrins to DNA. In general, metal derivatives of TMPyP having one or two axial ligands such as V(IV)=O[42,43] or Co(III)[44,45] do not intercalate, whereas those without axial ligand[46−48] such as Cu(II), Ni(II), or Au(III) do intercalate at GC-rich regions of DNA. It was reported that Co(III)-TMPyP binds outside of the DNA near the minor groove.[45]

Cationic porphyrins are occasionally used as an acceptor in DNA-mediated energy transfer because of their wide absorption range. TMPyP and its Ni(II) and Zn(II) derivatives quenched the fluorescence of DNA-intercalated ethidium.[49] Porphyrins were capable of efficiently quenching the fluorescence of an excited ethidium ion at a distance of 25−30 Å in the presence of DNA. The excited energy of 4′,6-diamidino-2-phenylindole, which bind preferentially at the minor groove of a continuous AT sequence, also transferred to TMPyP when they bind simultaneously to poly(dA)·poly(dT) and poly[d(A-T)$_2$].[24] The energy transfer of Förster type was suggested to be the mechanism in both cases.

In this study, we first systematically determined the binding geometry of various metallo- and nonmetallo-porphyrins using polarized light spectroscopy namely, circular and linear dichroism (CD and LD). The central metal in metallo-porphyrins included Cu(II), Ni(II), V(IV)=O, Ti(IV)=O, and Co(III) (Figure 1). Cu- and Ni-TMPyP lack the axial ligands and are plannar thus, expected to intercalate between DNA base-pairs. V(IV)=O and Ti(IV)=O are five coordinated and Co(III) six, which therefore they bind outside of the DNA. The efficiency as an energy acceptor of these porphyrins for the excited DNA-intercalated ethidium was also investigated and results were elucidated by resonance energy transfer which may be affected by three main factors, namely, the distance between acceptor and donor, relative orientation, and the spectral overlap reflecting the degree of transition coupling.

EXPERIMENTAL SECTION

Chemicals. TMPyP, NiTMPyP, and TiOTMPyP were purchased from Frontier Scientific, Inc. (Utah, U.S.A.). CoTMPyP and CuTMPyP were from Midcentury (Chicago, IL) and VOTMPyP from Porphyrin Products (Logan, Utah). Porphyrins were used without further purification. Native calf thymus DNA was purchased from Worthington (Lakewood, NJ). DNA was dissolved in 5 mM cacodylate buffer, pH 7.0, by exhaustive shaking at 4 °C, and this buffer was used throughout this study. Concentrations of porphyrins were spectrophotomatrically determined using molar extinction coefficients: $\varepsilon_{421\ nm}$ = 2.45 × 10^5 M^{-1} cm^{-1}, $\varepsilon_{418\ nm}$ = 1.50 × 10^5 M^{-1} cm^{-1}, $\varepsilon_{424\ nm}$ = 2.31 × 10^5 M^{-1} cm^{-1}, $\varepsilon_{438\ nm}$ = 2.07 × 10^5 M^{-1} cm^{-1}, $\varepsilon_{436\ nm}$ = 1.50 × 10^5 M^{-1} cm^{-1}, and $\varepsilon_{434\ nm}$ = 2.15 × 10^5 M^{-1} cm^{-1}, for metal-free TMPyP, NiTMPyP, CuTMPyP, VOTMPyP, TiOTMPyP, and CoTMPyP, respectively.[50,51] The molar extinction coefficient used for DNA was $\varepsilon_{260\ nm}$ = 6700 M^{-1} cm^{-1}. All measurements were performed at an ambient temperature.

Absorption and CD Spectra. Absorption spectra were recorded using a Cary 100 spectrophotometer (Palo Alto, CA). CD spectra were obtained using either a Jasco J-715 or a J-810 spectropolarimeter (Tokyo, Japan).

LD Spectrum. LD spectrum has been proven to be a powerful tool to determine the binding mode of DNA-bound drug. LD spectrum, which is defined by the difference in absorption spectrum between the polarized perpendicularly and in parallel with respect to the orientated sample, were measured on either J-715 or J-810 spectropolarimeter.[51,52] A Wada-type inner rotating flow cell was used to align DNA samples as described elsewhere. The measured LD was divided by isotropic absorption spectrum to calculate a dimensionless quantity, reduced LD spectrum (LD^r). LD^r spectrum is related to the angle (α) of the electric transition moment of DNA bases and DNA-bound drug with respect to the local DNA helix axis, and the ability of orientation (S) of the DNA-drug complex through:

$$\mathrm{LD}^r = \frac{\mathrm{LD}}{A_{\mathrm{iso}}} = 1.5S(\langle 3\cos^2\alpha \rangle - 1) \quad (1)$$

The orientation factor, S, can be determined from the magnitude of LD^r at 260 nm by assuming the average angle of electric transition of the in-plane DNA bases relative to the DNA helix axis as 86°. Once orientation factor is determined, the angle of the electric transition moment of DNA-bound drug can be easily calculated using eq 1.

Fluorescence Measurements. Fluorescence spectra were recorded using a Jasco FP-777 fluorometer. Excitation and emission wavelengths of 512 and 601 nm, respectively, were used in the fluorescence quenching experiment. The fluorescence quenching of DNA-bound ethidium by porphyrins were analyzed through Stern−Volmer plots.[53]

$$\frac{F_0}{F} = 1 + K_{SV}[Q] \quad (2)$$

In this equation, F_0 and F denote the fluorescence intensities of the fluorophore (the DNA-bound ethidium) in the absence and presence of quenchers, respectively. [Q] is the concentration of quencher, porphyrins and K_{SV} is the quenching constant.

RESULTS

Absorption and CD Spectra of Porphyrins. A large red-shift and hypochromism in absorption spectrum of any drug upon intercalation between DNA base-pairs may be a result of increasing the $\pi-\pi$ interaction and the change in drug's environment. In minor groove binding drug cases, changes in absorption spectrum usually relate to the change in the drug's conformation. Figure 2 depicts the absorption spectrum of various porphyrins in the presence and absence of DNA. The concentration of DNA for this series of measurements was 100 μM, and that of porphyrins were 0.5, 1.0, 1.5, 2.0, and 2.5 μM.

dx.doi.org/10.1021/jp212291r | J. Phys. Chem. B 2012, 116, 2330−2337

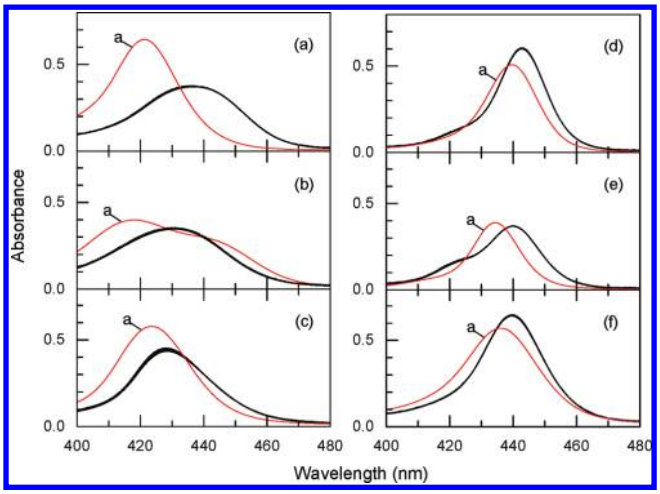

Figure 2. Absorption spectra of TMPyP of in the presence and absence of DNA (panel a), and that for M-TMPyPs. From panels b to f, M = Ni, Cu, VO, TiO, and Co. [Porphyrin] = 0.5, 1.0, 1.5, 2.0, and 2.5 μM and [DNA] = 100 μM. The spectra were normalized to the highest porphyrin concentration for easy comparison. Red curves (marked by a) in each panel indicate absorption spectra of porphyrin in the absence of DNA.

The resulting absorption spectra were normalized to the highest concentration for ease of comparison. Shown in Figure 2, the absorption spectra of all porphyrins are similar below the [porphyrin]/[DNA] ratio less than 0.025, when they were normalized. This observation suggests that the binding modes of porphyrins are identical at a different mixing ratio and the contribution from unbound porphyrin to spectrum were negligible. The presence of 0.5 μM of ethidium did not alter the shape and intensity of absorption spectrum of porphyrins (data not shown). TMPyP (Figure 2, panel a) produces absorption maximum at 421 nm in 5 mM cacodylate buffer, pH 7.0. The maximum absorbance was decreased by ~42% and the wavelength shifted by 16 nm upon binding to DNA. These changes in absorption spectrum are typical for TMPyP. The ~28% hypochromism and 6 nm red-shift (from 423 to 429 nm) upon binding to DNA was observed for CuTMPyP (panel c). For NiTMPyP case (panel b), a maximum at 418 nm accompanied by a shoulder about 442 nm was apparent in the absence of DNA. Binding of NiTMPyP to DNA resulted in an absorption maximum at 431 nm (13 nm red-shift) and the absorbance decreased by ~13%. In contrast with TMPyP and those do not have the axial ligand, VOTMPyP (panel d) and CoTMPyP (panel f) exhibited hyperchromism. Hyperchromism and red-shift were ~15% and 5 nm (from 438 to 443 nm), respectively, for VOTMPyP and were ~12% and 4 nm (from 436 to 440 nm), respectively, for CoTMPyP. TiOTMPyP exhibited a 6 nm red-shift (from 434 to 440 nm) and ~5% decreased absorbance at its maximum upon binding to DNA (panel e). In absorption measurements, TMPyP, CuTMPyP, and NiTMPyP produced large hypochromism and red-shift in the absorption spectrum while those with axial ligands exhibited hyperchromism or similar absorbance and the extent of shift was less significant.

Binding of achiral porphyrins to DNA induces CD spectra, particularly in the Soret absorption region due to interactions between the electric transition moments of porphyrin and chirally arranged DNA bases. Figure 3 shows the CD spectra of the six porphyrins complexed with DNA. Similarly with the

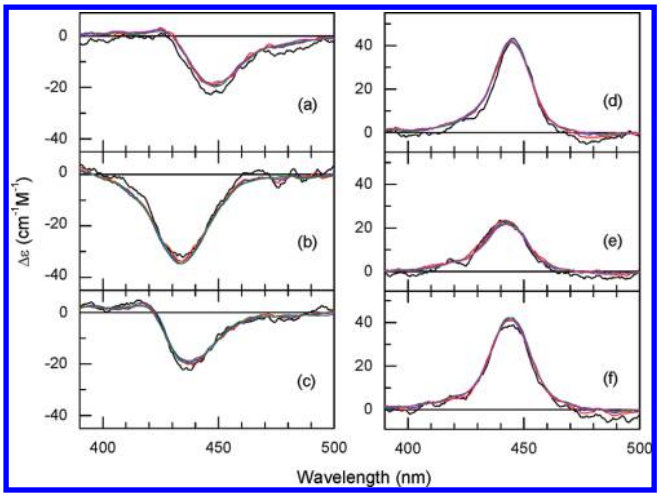

Figure 3. CD spectrum of DNA-bound porphyrins. Panel and curve assignment and the concentrations were the same as in Figure 2.

absorption spectra, appearance CD spectra were invariant of the [porphyrin]/[DNA] ratio adopted in this study. A similar negative CD band in the Soret region was apparent for TMPyP (panel a), NiTMPyP (panel b), and CuTMPyP (panel c) centered at 448, 433, and 437 nm, respectively. The magnitude of TMPyP and CuTMPyP were similar while that of NiTMPyP was slightly larger. The maximum negative CD of NiTMPyP and CuTMPyP appeared at shorter wavelength compared to that of TMPyP, conceivably due to the presence of central four-coordinated metals. In striking contrast, all porphyrins with axial ligands produced positive CDs with similar maximum wavelengths of 445, 443, and 444 nm for VOTMPyP, TiOTMPyP, and CoTMPyP, respectively. The magnitude at the maximum was similar for CoTMPyP- and VOTMPyP-DNA complexes but was smaller for the TiOTMPyP-DNA complex case. In addition to the absorption spectra, CD spectra were independent of the [porphyrin]/[DNA] ratio, suggesting a homogeneous binding mode at the mixing ratio adopted in this study. Finally, it should be noted that the presence of ethidium did not alter the CD spectrum for all the complexes, suggesting that the presence of intercalated ethidium did not interfere with the porphyrin intercalation.

LD and LD^r Spectra. LD spectra for the porphyrin-DNA complexes are depicted in Figure 4. In the DNA absorption region (~260 nm), a negative band was apparent as expected for the LD setup adopted in this study. A small decrease in the magnitude of LD in the DNA absorption region was observed for CuTMPyP (panel c) and CoTMPyP (panel f), and to a somewhat less extent for VOTMPyP (panel d). The shape of LD in this wavelength region was similar to the absorption spectrum except for the sign suggesting that the DNA conformation was not significantly altered. In addition to the absorption and CD spectra, the presence of ethidium (0.5 μM) did not affect the overall shape of the LD spectra in all complex cases: the concentration of ethidium was too low to have an effect. For TMPyP and porphyrins with no axial ligand cases, negative large LD signals appeared in the Soret region, which was proportional to porphyrin concentration. Porphyrins with axial ligands produced significantly smaller LD magnitudes in the Soret region when complexed with DNA. Negative LD in the Soret region for all porphyrin-DNA complexes suggested that the angle between the molecular plane of porphyrin and the local DNA helix was large.

dx.doi.org/10.1021/jp212291r | J. Phys. Chem. B 2012, 116, 2330–2337

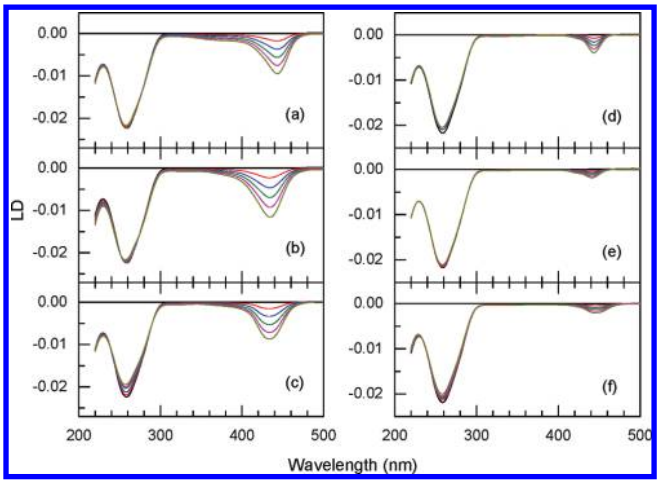

Figure 4. LD spectrum of the porphyrin-DNA complexes. The panel assignment and the concentrations are the same as in Figure 2, except that the spectra are not normalized.

Measured LD spectra were divided by normal absorption spectra to produce the LD^r spectrum which is related to the angle, α, between the electric transition moment of porphyrin and the DNA helix axis through eq 1. Calculated LD^r spectra are shown in Figure 5. The magnitude of negative LD^r in the

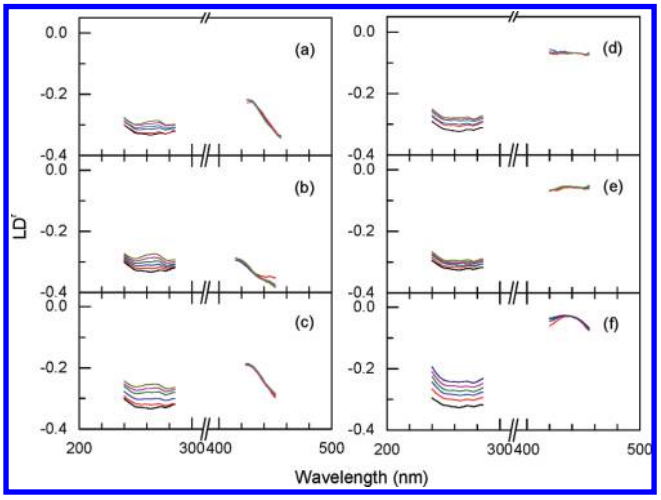

Figure 5. LD^r spectra of the porphyrin-DNA complexes obtained by division of measured LD (Figure 4) by absorption spectrum (Figure 2).

DNA absorption region decreased in all complexes suggesting that binding of porphyrin resulted in a kink or bending of DNA near binding site. Closer investigation revealed a small positive contribution which increased with increasing porphyrin concentration for the TMPyP-, NiTMPyP-, and CuTMPyP-DNA complexes as shown in panels a–c, respectively (Figure 5). This result suggested that at least some of the porphyrin's electric transition in this wavelength region tilted in a large extent from the DNA base plane. In the Soret absorption band, the planar porphyrins namely, TMPyP (panel a), NiTMPyP (panel b), and CuTMPyP (panel c), produced wavelength-dependent LD^r spectra. The LD^r magnitudes were comparable or larger than that in the DNA absorption region, which is typical for intercalated drugs.[54] The strong wavelength dependency suggested that either one of the B_x or B_y electric transition moments tilted strongly with respect to the DNA base plane. The LD^r values are lower than that in the DNA absorption region for the CuTMPyP-DNA complex in the entire Soret band (Figure 5, panel 3), which allowed for calculation of the angle of the B_x and B_y transitions with respect to the DNA helix axis by assuming 86° between the DNA base plane and the local DNA helix axis. The angles were 68° and 79°, respectively, suggesting that the molecular plane of CuTMPyP was skewed to a large extent in the intercalation pocket. For the TMPyP- and NiTMPyP-DNA complexes (Figure 5, panel a and b, respectively), the larger LD^r magnitudes at the maximum compared to those in the DNA absorption region, which prevented the calculation of the angle, α, because an imaginary number was involved in the calculation process. Hence, in these complex cases, one of the porphyrin's electric transition moment (assigned to B_y transition), which correspond to the maximum LD^r value was assumed to be 86° with respect to the local DNA helix axis in order to calculate the tilt angle of the DNA base plan and the B_x transition moment of porphyrin according to eq 1. The angle between B_y transition and the DNA base plane was 4° and 9° for TMPyP and NiTMPyP, respectively. That for CuTMPyP was 7°. The angle of B_x transitions were 16° for TMPyP and 12° for NiTMPyP relative to the B_y transition in the intercalation pocket; this angle for CuTMPyP was 11°. These results indicated that when one of the porphyrin's electric transition moment was assumed to be 86°, the angle, α, of the other transitions are 70°, 74° and 75°, respectively, for TMPyP, NiTMPyP and CuTMPyP. These results sre summarized in Table 1. In contrast, the porphyrins

Table 1. Angles α and β Calculated from LD^r, the Energy Transfer Distance σ, and the Relative Extent of Spectral Overlap[a]

			σ		
porphyrin	α	β	base pairs	Å	relative area of spectral overlap
TMPyP	70°		9.8	33.3	1
NiTMPyP	74°		8.0	27.2	0.85
CuTMPyP	75°		8.0	27.2	0.92
VOTMPyP	60°	44°	11.3	38.4	1.23
TiOTMPyP	56°–57°	41°–42°	6.6	22.4	0.86
CoTMPyP	59°–61°	39°–46°	17.6	59.8	1.46

[a]Angles α for the planar porphyrins were obtained by assuming 86° for one of the transition moments with respect to the local helix axis corresponding to the maximum LD^r value, while for those with axial ligands were calculated from the minimum and maximum LD^r values. Angles β were obtained by replacing $\cos^2\alpha$ in eq 1 with $1/2(\cos^2\beta)$ for the degenerate state. The symbol, σ, denotes the minimum distance in base pairs between ethidium and porphyrin required for complete quenching and the amount of relative spectral overlap was normalized to TMPyP.

with axial ligands showed significantly smaller LD^r magnitude in the Soret band. Panels d–f in Figure 5 show the LD^r spectra of VOTMPyP, TiOTMPyP and CoTMPyP complexed with DNA, respectively. The wavelength-dependency was less pronounced for these porphyrins, suggesting that in-plane $\pi^* \leftarrow \pi$ transitions, i.e., the B_x and B_y electric transitions, are largely degenerated. In this case, the tile angle is obtained by replacing $\cos^2\alpha$ in eq 1 by $1/2(\cos^2\beta)$.[55] The angles α calculated from the minimum and maximum LD^r values according to eq 1 were 56°~61° for both the B_x or B_y electric

dx.doi.org/10.1021/jp212291r | J. Phys. Chem. B 2012, 116, 2330–2337

transitions moments for all porphyrins possessing axial ligands. These angles for the CoTMPyP-DNA complex coincide with reported values.[44] The angle β which probably reflect the real binding geometry more precisely for the CoTMPyP-DNA complex calculated from the minimum and maximum LD^r values were 39°~46°. The β angle for the TiOTMPyP-DNA complex was 41°~42° and 44° for the VOTMPyP-DNA complex. These angles coincide with the tilt angle of the grooves of DNA with respect to the DNA helix axis. These results are summarized in Table 1.

Fluorescence Quenching and Spectral Overlap. Increasing the concentrations of any porphyrin resulted in a decrease of the fluorescence intensities of ethidium which intercalated between DNA base-pairs. In the absence of DNA, the quenching efficiencies of the porphyrins were negligible (data not shown). Quenching of the fluorescence of DNA-bound ethidium by porphyrins is depicted in the Stern–Volmer plot format in which the ratios of the fluorescence intensity in the absence of porphyrin to its presence were plotted with respect to the porphyrin concentration according to eq 2 (Figure 6). All porphyrins exhibited upward bending curves in

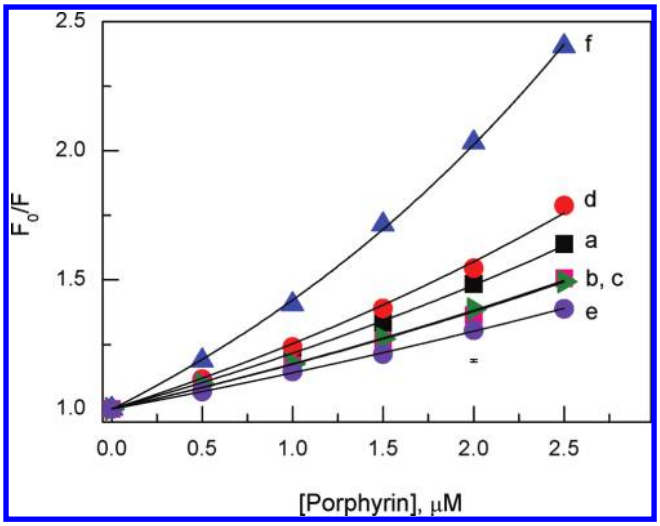

Figure 6. Stern–Volmer plots for the decrease in fluorescence intensity of DNA bound ethidium by various porphyrins. (a) TMPyP, (b, c) NiTMPyP ≈ CuTMPyP, (d) VOTMPyP, (e) TiOTMPyP, and (f) CoTMPyP. [DNA] = 100 μM and [ethidium] = 0.5 μM. The samples were excited at 512 nm and the emission wavelength was 601 nm. Slit widths were 5/5 nm for both excitation and emission. Representative error bars, denoting standard deviation from six measurements is also presented.

the Stern–Volmer plot suggesting the mechanism behind the quenching is neither a simple static nor dynamic process. The quenching efficiency is the highest for CoTMPyP: at a 2.5 μM concentration, more than 60% of ethidium fluorescence decreased with TiOTMPyP the least, being about 30% decrease. The quenching efficiencies for NiTMPyP and CuTMPyP were identical. The quenching efficiency of TMPyP was slightly higher than NiTMPyP and CuTMPyP, while that for VOTMPyP was between TMPyP and CoTMPyP. In short, the quenching efficiency became higher in the order of TiOTMPyP < NiTMPyP ≈ CuTMPyP < TMPyP < VOTMPyP < CoTMPyP. The results were fitted by the single exponential increase based on the one-dimensional resonance energy transfer[49] (see the Discussion) and the best-fit curves are also shown in Figure 6. Porphyrins absorb the radiation in a wide wavelength range in the UV–visible region suggesting the possibility of overlap between the emission spectrum of ethidium and the absorption spectrum of porphyrins. Therefore, the resonance energy transfer mechanism may contribute at least in part to the quenching of ethidium's fluorescence by porphyrins. Rescaled emission spectrum of DNA-bound ethidium and absorption spectrum of porphyrin that also were bound to DNA are depicted for selected porphyrins (Figure 7). Some of the absorption bands

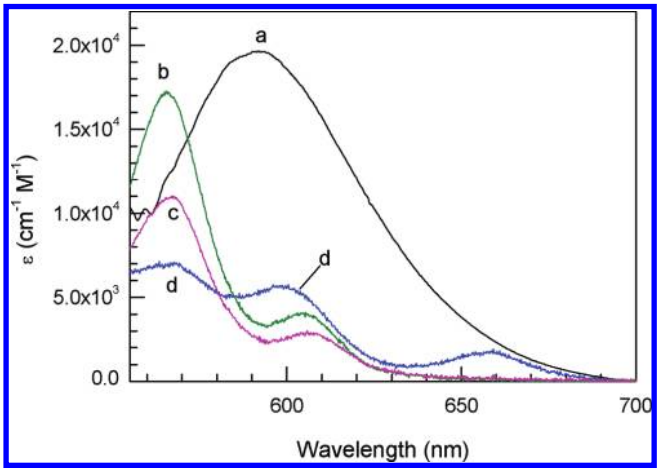

Figure 7. Rescaled emission spectra of the DNA-bound ethidium (curve a) and absorption spectra of selected porphyrins in the same wavelength region. VOTMPyP (curve b), TiOTMPyP (curve c), and TMPyP (curve d).

for porphyrins (Q_x and Q_y bands) overlapped with the emission spectrum of DNA-bound ethidium. The extents of the common area under the emission spectrum of ethidium and the absorption spectra of porphyrins were calculated relative to TMPyP. The values were 0.85, 0.86, 0.92, 1, 1.23, and 1.46 for NiTMPyP, TiOTMPyP, CuTMPyP, TMPyP, VOTMPyP, and CoTMPyP, respectively (Table 1). The order of the increasing the area roughly coincided with that of the quenching efficiency

DISCUSSION

Binding Geometry of Porphyrins. The appearance of spectra of the planar porphyrins including TMPyP, NiTMPyP, and CuTMPyP were characterized by a large red-shift and hypochromism in their absorption spectrum and a negative CD signal in the Soret absorption region. These spectral characteristics indicated that all porphyrins are intercalated between DNA base-pairs. In particular, the negative CD spectrum has been considered as a diagnostic for intercalated porphyrins.[16] On the other hand, increased or comparable intensity in absorbance were apparent for porphyrins with axial ligands. A positive CD was accompanied for all metallo-porphyrins with axial ligands. All these spectral changes indicated that the porphyrins with axial ligands bind outside of the DNA stem. The fact that the absorption and CD spectrum were retained at various [porphyrin]/[DNA] ratios indicated that the binding mode is homogeneous in the concentration range adopted in this study. When the population of porphyrin increases relative to the DNA concentration, stacking interaction between DNA-bound porphyrins occurs producing, in general, a bisignate CD spectrum. Any evidence for the stacking of porphyrins was not

dx.doi.org/10.1021/jp212291r | J. Phys. Chem. B 2012, 116, 2330–2337

found in the low range of [porphyrin]/[DNA] ratios adopted in this study.

The binding geometry can be classified into two types. In the Soret band, the two electric transition moments namely B_x and B_y transitions are degenerated. Upon binding to DNA, degeneracy may be partially removed by two reasons: change in the environment of transitions and difference in the angles of the transition moments relative to the local helix axis of DNA. The latter may be the main reason for the large wavelength-dependent tilt in the LD^r spectrum in the Soret absorption region that was observed for the planar porphyrins including TMPyP, NiTMPyP and CuTMPyP which have been known to intercalate between DNA base-pairs. The angles of the B_x and B_y transitions relative to the DNA helix axis cannot be calculated accurately because degeneracy of these two transitions are not completely removed and hence, the LD spectrum as well as absorption spectrum corresponding to each transition cannot be separated. However, the angles calculated from minimum and maximum LD^r values may provide a clue for the binding geometry. The difference in the angles of the B_x and B_y transitions relative to the DNA helix axis are 16°, 12°, and 11° for TMPyP, NiTMPyP, and CuTMPyP, respectively, suggesting that the molecular plane of these planar porphyrin are skewed to a large extent in the intercalation pocket. The extent of skews for those porphyrins possessing the four coordinated central metals namely, CuTMPyP and NiTMPyP are slightly less than TMPyP, conceivably due to the rigidness provided by the central metal. The average angles of the DNA base-pair plane were also somewhat tilted. The fact that the DNA bases as well as the porphyrin's molecular plane are skewed near the intercalation site is deviated from that observed for the three classical intercalators.

Whereas the α angle between the electric transition moment of porphyrin and the local DNA helix axis of porphyrins with an axial ligand lies bwtween 56°~61°, the β angles which conceivably reflect real angles in the complex were 39°~46° for CoTMPyP, 41°~42° for TiOTMPyP, and 44° for VOTMPyP. These angles are evidence that none of these porphyrins intercalate as it was expected from the presence of axial ligands which prevent intercalative binding mode due to steric hindrance. Thus, the possible binding site for porphyrins with axial ligands is one of the DNA grooves. A recent study provided evidence that the binding site for CoTMPyP to synthetic polynucleotides was the minor groove.[57] The CD and LD spectra of CoTMPyP complexed with poly(dA)·poly(dT) duplex resembled those bound to the poly(dA)·$[poly(dT)]_2$ triplex. Similar CD and LD spectra were also found for CoTMPyP complexed with poly(dG)·poly(dC) duplex and poly(dG)·poly(dC)·$poly(dC)^+$ triplex. Considering that the third poly(dT) or $poly(dC)^+$ strand binds parallel to the template poly(dA) and poly(dG), providing the steric hindrance at the major groove, these similarities indicated that CoTMPyP was located at the minor groove. Thus, in the current case, CoTMPyP conceivably binds primarily at the minor groove of DNA. At the minor groove, three possible binding modes for CoTMPyP may be considered. One of the possibilities is that the crescent shape side of this porphyrin fits deep along the minor groove. However, this binding mode is not conceivable because of the steric hindrance provided by the axial ligand. Other possibilities are that CoTMPyP either binds across the minor groove or the molecular plane of porphyrin faces the DNA bases. Although these two possibilities cannot be discriminated from the result presented in this study, TMPyP was suggested to be binding across the minor groove of poly[$d(A\text{-}T)_2$] with similar binding geometry[24] that was observed from this study. Considering that the appearance of the CD and LD spectra of VOTMPyP and TiOTMPyP resemble CoTMPyP when bound to DNA, the binding mode of the former two metalloporphyrins may be similar.

Energy Transfer from Ethidium to Porphyrins. When the emission energy level of a fluorophore is superimposed with the absorption energy level of an acceptor, the excited energy of the donor can be directly transferred to the acceptor, known as "Förster type resonance energy transfer (FRET)". The rate of FRET from the donor to the acceptor is proportional to the sixth power of the distance between donor and acceptor, R_0, determined by the following equation:[54,58,59]

$$R_0^6 = (J(\lambda)\kappa^2 Q_D n^{-4}) 8.79 \times 10^{-25} \text{ in cm}^6 \quad (3)$$

where $J(\lambda)$ denotes the spectral overlap between the emission spectrum of the donor and the absorption spectrum of the acceptor, κ is the relative orientation between the transition dipoles of the donor and the acceptor, Q_D is the quantum yield of the donor molecule in the absence of the acceptor, and n represents the refractive index of the medium. In eq 3, $J(\lambda)$ is the spectral overlap between the emission spectrum of the donor and absorption spectrum of the acceptor is determined by the following equation:

$$J(\lambda) = \int_0^\infty F_D(\lambda)\varepsilon_A(\lambda)\lambda^4 \, d\lambda \quad (4)$$

In this equation, $F_D(\lambda)$ is the normalized fluorescence intensity of the donor and $\varepsilon_A(\lambda)$ denotes the molar extinction coefficient of the acceptor. In the current case, the factors Q_D and n are identical for all porphyrins. The only factors that determine the efficiency of FRET is the spectral overlap and the orientation factor. When both acceptor and donor are bound to DNA, FRET can be assumed to occur in one dimension, through DNA. In this case, the quenching efficiency is reduced to eq 4.[49]

$$\frac{F_0}{F} = \exp\left(\frac{2\sigma[Q]}{[DNA] - 2[E^+]}\right) \quad (5)$$

where [Q] denotes the concentration of porphyrin and $[E^+]$ is the concentration of ethidium. The symbol σ is the minimum distance in base pairs (~3.4 Å per base pair) between ethidium and porphyrin required to permit the excited ethidium to emit a photon. From the results shown in Figure 6, the distances, σ, were calculated and are summarized in Table 1. The σ value was 9.8 base-pairs or ~33 Å for TMPyP which is slightly longer than the reported value of 25−30 Å by Pasternack and his co-workers,[49] conceivably due to different experimental conditions. The salt concentration in Pastenack's study was higher than that in this study, which provides more flexibility to DNA, resulting in a slightly shorter σ value. When the σ values are plotted with respect to the relative extent of the spectral overlap for various porphyrins (Figure 8), proportionality between these two are found; for CoTMPyP, which has the largest spectral overlap, the excited energy of ethidium can transfer to CoTMPyP over 17.8 base-pairs when they are simultaneously bound to DNA, while that for TiOTMPyP is the shortest, being 6.6 base-pairs. The spectral overlap of TiOTMPyP was the smallest.

The orientation factor, κ_2, can range from 0 to 4,[54] depending on the relative orientation of the donor and

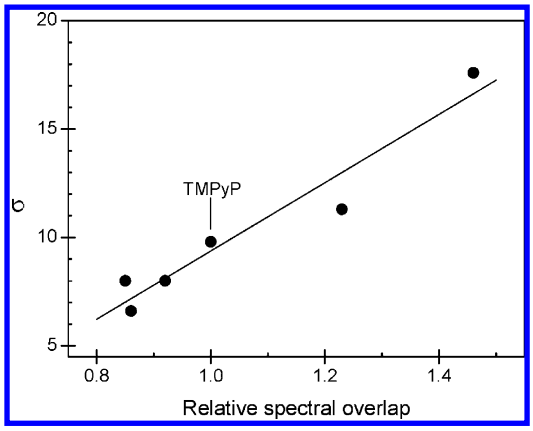

Figure 8. Plots for σ, the distance for complete fluorescence quenching with respect to the relative spectral overlap.

acceptor molecules. When they are oriented parallel head-to-tail $\kappa_2 = 4$, and when oriented in parallel $\kappa_2 = 1$. The variation of κ_2 from 1 to 4 contributes to differences in distance of only 26% because the sixth root of this factor is considered (eq 3). Furthermore, the σ values are 6.6, 11.3, and 17.8 for TiOTMPyP, VOTMPyP, and CoTMPyP, respectively, in spite of the binding geometries, and therefore relative orientations, of these porphyrins to DNA are similar. The planar porphyrins, which are intercalated between DNA base-pairs, resulted in σ values of 8.0, 8.0, and 9.8 respectively for NiTMPyP, CuTMPyP, and TMPyP. At least one of the B_x and B_y transition moments of these porphyrin is near parallel to the ethidium's transition dipole. From this geometry, more efficient energy transfer would be expected but it is not the case. Thus, the orientation factor is not a primary factor in determining the distance of energy transfer in the current porphyrin-ethidium-DNA system.

CONCLUSION

Both nonmetallo- and metallo planar porphyrins intercalate between DNA base-pairs. In the intercalation pocket, the molecular plane of porphyrin is skewed to a large extent. Porphyrins with axial ligands bind outside of DNA probably at the minor groove with tilt angles of 39°−46° between transition moments of the porphyrin and the local DNA helix axis. All porphyrins are effective acceptors for the excited energy of intercalated ethidium. The primary factor to determine the efficiency of energy transfer is the extent of spectral overlap between emission spectrum of ethidium and the absorption spectrum of porphyrins.

AUTHOR INFORMATION

Corresponding Author

*E mail: seogkim@yu.ac.kr. Tel: +82 53 810 2362. Fax: +82 53 815 5412.

Notes

The authors declare no competing financial interest.

ACKNOWLEDGMENTS

This work was supported by National Research Foundation of Republic of Korea (Grant Nos. NRF 2011-0014336 and NRF 2009-0087304).

REFERENCES

(1) Pasternack, R. F.; Gibbs, E. J.; Villafranca, J. J. *Biochemistry* **1983**, *22*, 2406−2414.
(2) Fiel, R. J.; Howard, J. C.; Datta-Gupta, N. *Nucleic Acid Res.* **1979**, *6*, 3093−3118.
(3) Fiel, R. J.; Datta-Gupta, N.; Mark, E. H.; Howard, J. C. *Cancer Res.* **1981**, *41*, 3543−3545.
(4) Fiel, R. J.; Beerman, T. A.; Mark, E. H.; Datta-Gupta, N. *Biochem. Biophys. Res. Commun.* **1982**, *107*, 1067−1074.
(5) Robertson, C. A.; Evans, H. D.; Abrahamse, H. *J. Photochem. Photobiol. B* **2009**, *96*, 1−8.
(6) Vicente, M. G. *Curr. Med. Chem. Anti-Canc. Agents* **2001**, *1*, 175−194.
(7) Timothy, J.; Jensen, M.; Vicente, G. H.; Luguya, R.; Norton, J.; Fronczek, F. R.; Smith, K. M. *J. Photochem. Photobiol. B* **2010**, *100*, 100−111.
(8) Vicente, M. G. *Curr. Med. Chem. Anti-Canc. Agents.* **2001**, *1*, 175−194.
(9) de Oliveira Silva, F. R.; Bellini, M. H.; Nabeshima, C. T.; Schor, N.; Vieira, N. D. Jr.; Courrol, L. C. *Photodiagn. Photodyn.* **2011**, *8*, 7−13.
(10) Ding, L.; Balzarini, J.; Schols, D.; Meunier, B.; Clercq, E. *Biochem. Pharmacol.* **1992**, *44*, 1675−1679.
(11) Zhao, P.; Xu, L.-C.; Huang, J.-W.; Zheng, K.-C.; Fu, B.; Yu, H.-C.; Ji, L.-N. *Biophys. Chem.* **2008**, *135*, 102−109.
(12) Zhao, P.; Xu, L.-C.; Huang, J.-W.; Zheng, K.-C.; Liu, J.; Yu, H.-C.; Ji, L. N. *Biophys. Chem.* **2008**, *134*, 72−83.
(13) Zhao, P.; Xu, L.-C.; Huang, J.-W.; Fu, B.; Yu, H.-C.; Zhang, W.-H.; Chen, J.; Yao, J.-H.; Ji, L. N. *Bioorg. Chem.* **2008**, *36*, 278−287.
(14) Marzilli, L. G.; Banville, L. D.; Zon, G.; Wilson, W. D. *J. Am. Chem. Soc.* **1986**, *108*, 4188−4192.
(15) Guliaev, A. B.; Leontis, N. B. *Biochemistry* **1999**, *38*, 15425−15437.
(16) Lee, Y.-A.; Lee, S.; Cho, T.-S.; Kim, C.; Han, S. W.; Kim, S. K. *J. Phys. Chem. B* **2002**, *106*, 11351−11355.
(17) Strickland, J. A.; Marzilli, L. G.; Wilson, W. D. *Biopolymers* **1990**, *29*, 1307−1323.
(18) Schneider, H.-J.; Wang, M. *J. Org. Chem.* **1994**, *59*, 7473−7478.
(19) Sehlstedt, U.; Kim, S. K.; Carter, P.; Goodisman, J.; Vollano, J. F.; Nordén, B.; Dabrowiak, J. C. *Biochemistry* **1994**, *33*, 417−426.
(20) Pasternack, R. F.; Goldsmith, J. I.; Gibbs, E. J. *Biophys. J.* **1998**, *75*, 1024−1031.
(21) Yun, B. H.; Jeon, S. H.; Cho, T.-S.; Yi, S. Y.; Sehlstedt, U.; Kim, S. K. *Biophys. Chem.* **1998**, *70*, 1−10.
(22) Lee, S.; Jeon, S. H.; Kim, B.-J.; Han, S. W.; Jang, H. G.; Kim, S. K. *Biophys. Chem.* **2001**, *92*, 35−45.
(23) Park, T.; Kim, J. M.; Han, S. W.; Lee, D.-J.; Kim, S. K. *Biochim. Biophys. Acta* **2005**, *1726*, 287−292.
(24) Jin, B.; Lee, H. M.; Lee, Y.-A.; Ko, J. H.; Kim, C.; Kim, S. K. *J. Am. Chem. Soc.* **2005**, *127*, 2417−2424.
(25) Carvlin, M. J.; Datta-Gupta, N.; Fiel, R. J. *Biochem. Piophys. Res. Commun.* **1982**, *108*, 66−73.
(26) Carvlin, M. J.; Fiel, R. J. *Nucleic Acids Res.* **1983**, *11*, 6121−6139.
(27) Banville, D. L.; Marzilli, J. A.; Strickland, J. A.; Wilson, W. D. *Biopolymers* **1986**, *25*, 1837−1858.
(28) LeDoan, T.; Perrouault, C.; Chassignol, M.; Thung, N. T.; Hélène, C. *Nucleic Acids Res.* **1987**, *15*, 8643−8659.
(29) Mukundan, N. E.; Pethö, G.; Dixon, D. W.; Kim, M. S.; Marzilli, L. G. *Inorg. Chem.* **1994**, *33*, 4676−4687.
(30) Mukundan, N. E.; Pethö, G.; Dixon, D. W.; Marzilli, L. G. *Inorg. Chem.* **1995**, *34*, 3677−3687.
(31) Pasternack, R. F.; Giannetto, A.; Pagano, P.; Gibbs, E. J. *J. Am. Chem. Soc.* **1991**, *113*, 7799−7800.
(32) Pasternack, R. F.; Bustamante, C.; Collings, P. J.; Giannetto, A.; Gibbs, E. J. *J. Am. Chem. Soc.* **1993**, *115*, 5393−5399.
(33) Mallamace, F.; Micali, N.; Monsu'Scolaro, L.; Pasternack, R. F.; Romeo, A.; Terracina, A.; Trusso, S. J. *J. Mol. Struct.* **1996**, *383*, 255−260.

(34) Pasternack, R. F.; Gibbs, E. J.; Collings, P. J.; dePaula, J. C.; Turzo, L. C.; Terracina, A. *J. Am. Chem. Soc.* **1998**, *120*, 5873−5878.
(35) Pasternack, R. F.; Gibbs, E. J.; Bruzewicz, D.; Stewart, D.; Engstrom, K. S. *J. Am. Chem. Soc.* **2002**, *124*, 3533−3539.
(36) Pasternack, R. F. *Chirality* **2003**, *15*, 329−332.
(37) Scolaro, L. M.; Romeo, A.; Pasternack, R. *J. Am. Chem. Soc.* **2004**, *126*, 7178−7179.
(38) Lee, Y.-A.; Kim, J.-O.; Cho, T.-S.; Song, R.; Kim, S. K. *J. Am. Chem. Soc.* **2003**, *125*, 8106−8107.
(39) Kim, J.-O.; Lee, Y.-A.; Yun, B. H.; Han, S. W.; Kwaq, S. T.; Kim, S. K. *Biophys. J.* **2004**, *86*, 1012−1017.
(40) Jin, B.; Ahn, J. E.; Ko, J. K.; Wang, W.; Han, S. W.; Kim, S. K. *J. Phys. Chem. B* **2008**, *112*, 15875−15882.
(41) Jung, J.-A.; Lee, S. H.; Jin, B.; Sohn, Y.; Kim, S. K. *J. Phys. Chem. B* **2010**, *114*, 7641−7648.
(42) Park, T. G.; Ko, J. H.; Ryoo, A. Y.; Kim, J.-M.; Cho, D. W.; Kim, S. K. *Biochem. Biophys. Acta* **2006**, *1760*, 388−394.
(43) Cho, D. W.; Jeong, D. H.; Ko, J. H.; Kim, S. K.; Yoon, M. *J. Photochem. Photobiol. A: Chem.* **2005**, *174*, 207−313.
(44) Sehlstedt, U.; Kim, S. K.; Carter, P.; Soodisman, J.; Vollano, J. F.; Nordén, B.; Dabrowiak, J. C. *Biochemistry* **1994**, *33*, 417−426.
(45) Jin, B.; Shin, J. S.; Bae, C. H.; Kim, J.-M.; Kim, S. K. *Biochem. Biophys. Acta* **2006**, *1760*, 993−1000.
(46) Dougherty, G.; Pasternack, R. F. *Biophys. Chem.* **1992**, *44*, 11−19.
(47) Nyarko, E.; Hanada, N.; Habib, A.; Tabata, M. *Inorg. Chim. Acta* **2004**, *357*, 739−745.
(48) Lee, M. J.; Lee, G.-J.; Lee, D.-J.; Kim, S. K.; Kim, J.-M. *Bull. Korean Chem. Soc.* **2005**, *26*, 1728−1734.
(49) Pasternack, R. F.; Caccam, M.; Keogh, B.; Stephenson, T. A.; Williams, A. P.; Gibbs, E. J. *J. Am. Chem. Soc.* **1991**, *113*, 6835−6840.
(50) Lin, M.; Lee, M.; Yue, K. T.; Marzilli, L. G. *Inorg. Chem.* **1993**, *32*, 3217−3226.
(51) Lu, M.; Guo, Q.; Pasternack, R. F.; Wink, D. J.; Seeman, N. C.; Kallenbach, N. R. *Biochemistry* **1990**, *29*, 1614−1624.
(52) Nordén, B.; Kubista, M.; Kurucsev, T. *Q. Rev. Biophys. Chem.* **1992**, *25*, 51−170.
(53) Nordén, B.; Kurucsev, T. *J. Mol. Recognit.* **1994**, *7*, 141−156.
(54) Lakowiz, J. R. *Principles of Fluorescence Spectroscopy*, 3rd ed.; Springer: New York, 2006.
(55) Tuite, E.; Nordén, B. *Bioorg. Med. Chem.* **1995**, *3*, 701−711.
(56) Härd, B.; Nordén, B. *Biopolymers* **1986**, *25*, 1209−1228.
(57) Jin, B.; Shin, J. S.; Bae, C. H.; Kim, J.-M.; Kim, S. K. *Biochem. Biophys. Acta* **2006**, *1760*, 993−1000.
(58) Kang, J. S.; Lakowicz, J. R. *J. Biochem. Mol. Biol.* **2001**, *34*, 551−558.
(59) Malicka, J.; Gryczynski, I.; Fang, J.; Kusba, J.; Lakowicz, J. R. *Anal. Biochem.* **2003**, *315*, 160−169.